Multiple Cyclotron Method to Search for *CP* Violation in the Neutrino Sector

J. M. Conrad[1] and M. H. Shaevitz[2]

[1]*Department of Physics, Massachusetts Institute of Technology, Cambridge, Massachusetts 02139, USA*
[2]*Department of Physics, Columbia University, New York, New York 10027, USA*

(Received 15 January 2010; published 9 April 2010)

New low-cost, high-power proton cyclotrons open the opportunity for a novel precision search for *CP* violation in the light neutrino sector. The accelerators can produce decay-at-rest neutrino beams located at multiple distances from a Gd-doped ultralarge water Cherenkov detector in order to search for *CP* violation in $\bar{\nu}_\mu \to \bar{\nu}_e$ oscillations at short baselines. This new type of search complements presently proposed experiments, providing measurements that could lead to a substantially better exploration of *CP* violation in the neutrino sector.

DOI: 10.1103/PhysRevLett.104.141802 PACS numbers: 14.60.Pq, 11.30.Er, 14.60.St, 29.20.dg

I. Introduction.—With the discovery of neutrino oscillations, particle physicists have been inspired to develop theories that explain very light-neutrino masses. The most popular models invoke grand-unified-theory- (GUT-) scale Majorana partners which can decay, producing a matter-antimatter asymmetry in the early Universe through the mechanism of *CP* violation. Observation of *CP* violation in the light-neutrino sector would be a strong hint that this theory is correct.

To incorporate *CP* violation, the light-neutrino 3×3 mixing matrix is expanded to include a *CP* violating phase, δ_{CP}. Sensitivity to δ_{CP} comes through muon-to-electron flavor oscillations at the atmospheric mass-squared difference, Δm^2_{31}. The oscillation probability, neglecting matter effects, is given by [1]

$$\begin{aligned} P = {} & \sin^2\theta_{23}\sin^2 2\theta_{13}\sin^2\Delta_{13} \\ & \mp \sin\delta_{cp}\sin 2\theta_{13}\sin 2\theta_{23}\sin 2\theta_{12}\sin^2\Delta_{13}\sin\Delta_{12} \\ & + \cos\delta_{cp}\sin 2\theta_{13}\sin 2\theta_{23}\sin 2\theta_{12}\sin\Delta_{13}\cos\Delta_{13}\sin\Delta_{12} \\ & + \cos^2\theta_{23}\sin^2 2\theta_{12}\sin^2\Delta_{12}, \end{aligned} \quad (1)$$

where $\Delta_{ij} = \Delta m^2_{ij} L/4E_\nu$, and $-(+)$ refers to neutrinos (antineutrinos).

In Eq. (1), aside from δ_{CP}, all but two of the parameters (θ_{13} and the sign of Δm^2_{31}) are well known. Further precision on these known parameters is expected in the near future (see Table I). With respect to θ_{13}, global fits report a nonzero value at the $\sim 1\sigma$ level [2,5]. This parameter drives the amplitude for the *CP* violating terms in Eq. (1) and therefore sets the level of technical difficulty for observing *CP* violation. The unknown sign of Δm^2_{31}, referred to as "the mass hierarchy," affects the sign of term 3 in Eq. (1). Matter effects modify Eq. (1) and are sensitive to the mass hierarchy.

We propose a new method to search for *CP* violation which is unique in its reliance on a large antineutrino sample. This method uses antineutrino sources at multiple distances to illuminate a single detector. Nonzero values of δ_{CP} are observed through departures in the L and E dependence of the absolute appearance rates from the $\delta_{CP} = 0$ prediction of Eq. (1) (see Table I for input parameters).

The neutrino sources would be based on commercially-developed, small (2.5 m diameter), high-power proton cyclotron accelerators that are under development [7]. A 250 MeV, 1 mA cyclotron is under construction at MIT and a GeV-energy, megawatt-class cyclotron is presently under design. When in production, because of new, inexpensive superconducting technology, these machines are expected to cost 5% of a conventional proton accelerator (<20 M). These machines will demonstrate the beam physics and engineering needed for this experiment.

For this study, we assume accelerators that target 2 GeV protons at 2.5 mA during a 100 μs pulse every 500 μs, delivering 9.4×10^{22} protons per year to a beam stop. The result is a high-intensity, isotropic, decay-at-rest (DAR) neutrino beam arising from the stopped pion decay chain: $\pi^+ \to \nu_\mu + \mu^+$ followed by $\mu^+ \to e^+ \bar{\nu}_\mu \nu_e$. The flux, shown in Fig. 1, has an end point of 52.8 MeV. Each cyclotron produces 4×10^{22}/flavor/year of ν_e, ν_μ, and $\bar{\nu}_\mu$. The $\bar{\nu}_e$ fraction in the beam is very low ($\sim 10^{-4}$) because most π^- are captured before decay.

This experiment utilizes an ultralarge water Cherenkov detector such as Hyper-K [8], MEMPHYS [9], or the detector proposed for the Deep Underground Science and Engineering Laboratory (DUSEL) [10]. We use a 300 kton

TABLE I. Left: Present values and uncertainties for oscillation parameters, reported in the references. Right: Future expectations used in this study.

Parameter	Present:			Assumed Future:		
	Value	Uncert. (±)	Ref.	Value	Uncert. (±)	Ref.
$\Delta m^2_{21} \times 10^{-5}$ eV^2	7.65	0.23	[2]	7.65	···	···
$\Delta m^2_{31} \times 10^{-3}$ eV^2	2.40	0.12	[2]	2.40	0.02	[3]
$\sin^2(2\theta_{12})$	0.846	0.033	[2]	0.846	···	···
$\sin^2(2\theta_{23})$	1.00	0.02	[2]	1.00	0.005	[4]
$\sin^2(2\theta_{13})$	0.06	0.04	[5]	0.05	0.005	[6]

 © 2010 The American Physical Society

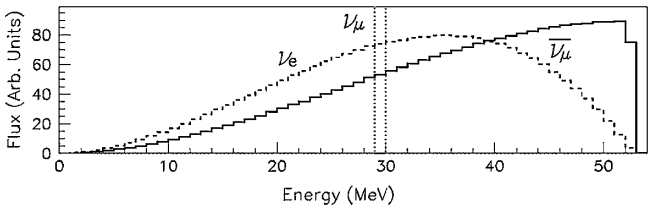

FIG. 1. Energy distribution of neutrinos in a DAR beam.

DUSEL detector as our model. Water provides a target of free protons for the inverse beta decay (IBD) interaction: $\bar{\nu}_e + p \rightarrow n + e^+$.

IBD interactions are identified via a coincidence signal. The first signal is from the Cherenkov ring produced by the positron. The second signal is from capture of the neutron. The signal from neutron capture on protons, which produces only a single 2.2 MeV γ, is too feeble to be efficiently observed in a large Cherenkov detector. For that reason, doping with gadolinium (Gd), which has a high capture rate and a short capture time, is proposed [11]. Neutron capture on Gd produces multiple photons totaling $\sim$8 MeV, which allows for observation at higher efficiency than undoped water. For this discussion, we assume that future water Cherenkov detectors can attain 67% efficiency, equal to that observed in Super-K tests [12]. Gd doping of water is under development [13]. In IBD events, the energy of the neutrino is related to the energy of the positron and kinetic energy of the neutron, K, by $E_{\bar{\nu}} = E_{e^+} + (M_n - M_p) + K$ [14].

The accelerators are placed at three separate baselines, L, for the $\bar{\nu}_\mu \rightarrow \bar{\nu}_e$ search (see Fig. 2). Each set of accelerators at the three sites runs for a 20% duty factor interspersed in time; the other 40% of the time is used to collect beam-off data. The longest baseline is $L = 20$ km, where $\sim$40 MeV $\bar{\nu}_\mu$ are at oscillation maximum for the measured value of Δm^2_{31}. In this case, term 2 of Eq. (1) will contribute while term 3 will not. A midbaseline accelerator site is

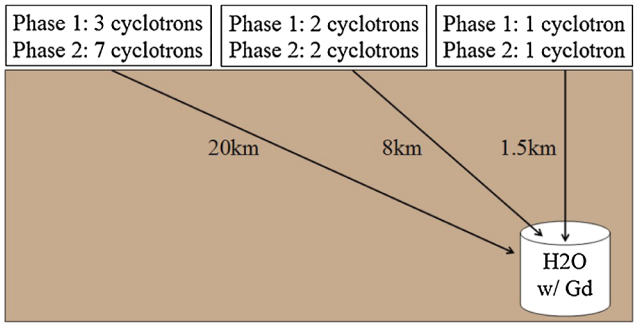

FIG. 2 (color online). Proposed experimental layout. Each phase corresponds to a 5-year data-taking period with each of the three source sites on for 20% of the time. (Phase 2 is an example; the number of cyclotrons will be optimized based on Phase 1 measurements.)

located at $L = 8$ km, where term 3 of Eq. (1) is nonzero. The shortest baseline accelerator site is at $L = 1.5$ km, directly above the DUSEL detector. At this location, the neutrino-electron elastic scattering rates are sufficient to allow precision measurement of the neutrino flux normalization as discussed below. We propose multiple accelerators at the various locations (see Fig. 2), which is feasible because of the low cost per machine. For the L of a given event to be well determined, the beams from each location are staggered in time.

Term 3 of Eq. (1) leads to an inherent ambiguity between δ_{CP} and the mass hierarchy. We assume that on the time scale of the measurements presented here, the mass hierarchy will be measured using LBNE [10] or atmospheric neutrino measurements [15]. For the sensitivity estimates, we choose the normal hierarchy as the example model.

We present a two-phase experiment, where the design has flexibility in the second phase. In our case, each phase represents five years. The first phase explores the oscillation space at $\sim 3\sigma$ and requires one accelerator at the near location, two at the midlocation and three at the far location. Once a signal for CP violation has been localized, the strategy for the second phase can be determined. As an example for phase 2, we have chosen a design with one, two, and seven accelerators. This design matches the sensitivity of a run of LBNE with 30×10^{20} protons on target in neutrino mode followed by 30×10^{20} protons on target in antineutrino mode [10].

This design is unique among proposals for CP violation searches and complementary to the present plans [6,10]. The measurement is done with antineutrinos, while all existing proposals rely heavily on neutrino data. The antineutrino flux uncertainties are different and well-controlled. Because of the low energy, the interaction systematics are also different. Varying L, while employing a single detector is novel and reduces systematics. A two-phase program which allows an optimized measurement strategy is powerful and potentially cost-saving.

II. Event types and backgrounds.—The energy range of the analysis is $20 < E_\nu < 55$ MeV. The lower cut renders potential backgrounds from radioactive decay and spallation negligible. The upper cut is chosen because of the 52.8 MeV signal endpoint.

In this energy range, three types of interactions must be considered. First is the IBD signal, with an estimated reconstruction efficiency of $\epsilon_{\text{recon}} = 67\%$, based on studies for Super-K [12]. Second is $\nu_e + \text{O} \rightarrow e^- + \text{F}$ ("ν_eO"), with a suppressed cross section relative to IBD due to nuclear effects [16,17] and no neutron capture. Third is neutrino-electron elastic scattering (νeES) $\nu_e + e^- \rightarrow \nu_e + e^-$. (This category also includes ν_μ and $\bar{\nu}_\mu$ elastic scattering on electrons which are 11% and 12% of the total, respectively.) This is separable from ν_eO by angular cuts [18,19] and, so, can be used for the flux normalization. For ν_eO and νeES events, we estimate $\epsilon_{\text{recon}} = 75\%$ [18].

Beam-off backgrounds arise from three sources: atmospheric $\nu_\mu p$ scatters with muons below Cherenkov threshold which stop and decay (''invisible muons''), atmospheric IBD events, and diffuse supernova neutrinos. These are all examples of correlated backgrounds; accidental beam-off backgrounds are estimated to be negligible. The rates of these correlated backgrounds are scaled from analyses for the GADZOOKS experiment [11]. The interaction rates of the beam-off backgrounds are well-measured during the 40% beam-off running fraction.

The beam-on backgrounds have both accidental and correlated sources. The accidental backgrounds arise from the ν_e in the beam which are followed by a neutron-like event. This background is estimated to be very small using the measurements from the Super-K Gd-doping study [12]. Correlated backgrounds are produced by the intrinsic $\bar{\nu}_e$ content of the beam. This is reduced by careful design of the beam stop. We assume a long water target embedded in a copper absorber, surrounded by steel for each cyclotron. We target at 100 degrees from the detector to reduce decay-in-flight (DIF) backgrounds. For 2 GeV protons on target, the pion yields, π^+/p (π^-/p), are 0.43 (0.056). with a π^+ (π^-) DIF fraction of 0.017 (0.025). The decays of μ^-'s are further reduced by a factor of 8.3 since the μ^- will be captured before decaying. The compact design decreases the $\bar{\nu}_e$ production compared to LAMPF/LANCE by a factor of 1.7. The beam has a $\bar{\nu}_e/\nu_e$ ratio of 4×10^{-4}.

III. Systematic errors.—The multiple-DAR-source design is an elegant choice for precision oscillation physics because the beam and detector systematics are low. The shape of the DAR flux with energy is known to high precision and is common among the various distances, thus shape comparisons will have small uncertainties. The neutrino flux from the three distances is accurately determined from the direct measurement of the π^+ production rate using νeES events from the near accelerator. Existing proton rate monitors assure that relative proton intensities are understood to 0.1%. The interaction and detector systematic errors are low since all events are detected in a single detector. The IBD cross section for the signal is well known [14]. The fiducial volume error on the IBD events is also small due to the extreme volume-to-surface-area ratio of the ultralarge detector.

The largest systematic errors arise from the νeES sample used to determine the absolute normalization of the flux. The error on this cross section is 0.5% due to a 0.7% uncertainty from the NuTeV $\sin^2\theta_W$ measurement [20]. We assume a 2.1% energy scale error [21] which leads to a 1% error on the DAR flux when a $E_{\rm vis} > 10$ MeV cut on the events is applied. The ν_e events on oxygen and IBD events with a missing neutron can be separated from the νeES sample since the angular distribution of νeES events is very forward-peaked, while these backgrounds have a broad distribution [19]. (For example, only 0.8% of the ν_e-oxygen events have $\cos\theta < 0.95$ giving a less than 4% background to the IBD sample.) We take the uncertainty from contamination by these events to be negligible. The uncertainty of the electron-to-free-proton ratio in water is also very small. Adding the νeES systematics in quadrature, the systematic error on the IBD flux is expected to be 1.1%. For the total error on the IBD flux, one must then add the νeES statistical error in quadrature, which depends on the running period.

The other significant systematic error is on the efficiency for neutron detection in IBD events. To reduce uncertainties, neutrons are tagged via timing rather than position reconstruction. This leads to an inefficiency for neutrons outside of the timing window with a systematic uncertainty goal of 0.5% [12].

TABLE II. Event samples for the combined two-phase run for $\sin^2 2\theta_{13} = 0.05$ and parameters from Table I (future).

Event Type	1.5 km	8 km	20 km
IBD Oscillation Events ($E_{\rm vis} > 20$ MeV)			
$\delta_{CP} = 0^0$, Normal Hierarchy	763	1270	1215
$\delta_{CP} = 0^0$, Inverted Hierarchy	452	820	1179
$\delta_{CP} = 90^0$, Normal Hierarchy	628	1220	1625
$\delta_{CP} = 90^0$, Inverted Hierarchy	628	1220	1642
$\delta_{CP} = 180^0$, Normal Hierarchy	452	818	1169
$\delta_{CP} = 180^0$, Inverted Hierarchy	764	1272	1225
$\delta_{CP} = 270^0$, Normal Hierarchy	588	870	756
$\delta_{CP} = 270^0$, Inverted Hierarchy	588	870	766
IBD from Intrinsic $\bar{\nu}_e$ ($E_{\rm vis} > 20$ MeV)	600	42	17
IBD Non-Beam ($E_{\rm vis} > 20$ MeV)			
atmospheric $\nu_\mu p$ ''invisible muons''	270	270	270
atmospheric IBD	55	55	55
diffuse SN neutrinos	23	23	23
$\nu - e$ Elastic ($E_{\rm vis} > 10$ MeV)	21 570	1516	605
ν_e Oxygen ($E_{\rm vis} > 20$ MeV)	101 218	7116	2840

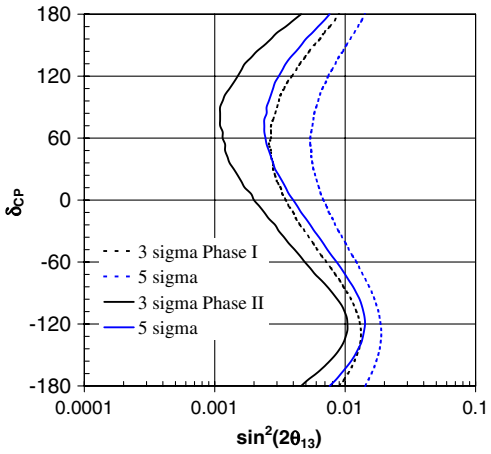

FIG. 3 (color online). Phase 1 and combined-phase sensitivity to $\theta_{13} \neq 0$ at 3σ and 5σ.

TABLE III. The 1σ measurement uncertainty on δ_{CP} for various values of $\sin^2\theta_{13}$ for the combined two-phase data. Top: Systematic and statistical errors. Bottom: Statistics only.

$\sin^2 2\theta_{13}/\delta_{CP}$	-180	-90	0	90	135
0.01	52.5	47.2	29.0	38.8	48.5
0.05	21.6	21.9	19.5	25.6	30.4
0.09	18.3	19.9	17.6	23.8	26.3
0.01	51.3	45.5	26.9	36.7	46.9
0.05	19.9	21.2	18.2	24.2	29.6
0.09	16.8	19.2	16.5	22.6	25.3

IV. Oscillation sensitivities.—Sensitivity estimates were made by calculating the χ^2 for a given set of predicted events and investigating the χ^2 minimization and excursion, using a method similar to Ref. [6]. Matter effects were included in the fit, but are negligible due to the short baseline. Systematic uncertainties (see Sec. and Table I) were constrained by pull-term contributions to the χ^2 of the form $(k_i - 1)^2/\sigma_i^2$, where σ_i^2 are the uncertainties. Results are given for two scenarios (see Fig. 2): Phase 1 and Phase 1 + 2 combined. Table II gives the event samples associated with the combined phases, for the various classes of oscillation, background, and calibration events.

The sensitivity for observing a nonzero value for θ_{13} at the 3 and 5σ CL as a function of δ_{CP} is shown in Fig. 3 for Phase 1 and Phase 1 + 2 running. This sensitivity meets that of LBNE, but is inverted in its δ_{CP} dependence [10].

The combined two-phase running yields a 4.1σ measurement of δ_{CP} at the test point of $\sin^2 2\theta_{13} = 0.05$ and $\delta_{CP} = -90^0$, as shown in Table III (top). The correlated measurement uncertainties are shown in Fig. 4 for 1 and 2σ contours. Table III (bottom), which provides the statistical uncertainty, indicates that the measurement is statistics limited.

V. Conclusions.—We have described a novel experiment to search for *CP* violation in the neutrino sector. This experiment is relatively low cost, employing multiple high-powered compact cyclotrons located at $L = 1.5$, 8, and 20 km from a large water Cherenkov detector. Using the example of the DUSEL detector, for $\sin^2 2\theta_{13} = 0.05$, the *CP* violation parameter δ_{CP} can be measured to the level of LBNE ($>4\sigma$) in a 2-phase 10-year run.

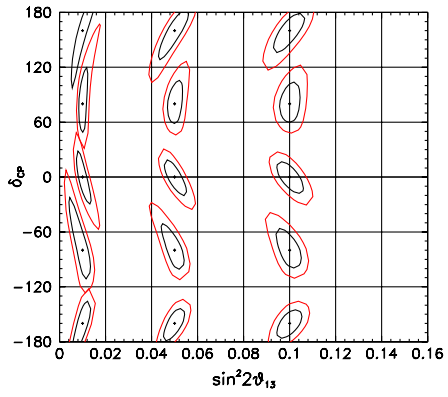

FIG. 4 (color online). Correlated sensitivity (1 and 2σ contours) to δ_{CP} and $\sin^2 2\theta_{13}$ for the combined two-phase running.

The complementary nature of this measurement makes it a compelling addition to the program. This experiment will probe for *CP* violation with antineutrinos, unlike the present program which relies heavily on neutrino interactions. The systematics are also quite different and low compared to present planned experiments. As a result, this experiment will provide a powerful input to our global search for new physics in the neutrino sector.

The authors thank the DAEδALUS group for discussions, especially Timothy Antaya, William Barletta, and William Louis. We thank the National Science Foundation for support.

[1] H. Nunokawa, S. J. Parke, and J. W. F. Valle, Prog. Part. Nucl. Phys. **60**, 338 (2008).
[2] T. Schwetz, M. A. Tortola, and J. W. F. Valle, New J. Phys. **10**, 113011 (2008).
[3] T. Schwetz, Acta Phys. Pol. B **36**, 3203 (2005).
[4] P. Huber, M. Lindner, T. Schwetz, and W. Winter, J. High Energy Phys. 11 (2009) 044.
[5] G. L. Fogli, E. Lisi, A. Marrone, A. Palazzo, and A. M. Rotunno, arXiv:0905.3549.
[6] K. B. M. Mahn and M. H. Shaevitz, Int. J. Mod. Phys. A **21**, 3825 (2006).
[7] For further information on the Gigatron, contact T. Antaya, NW22-139, 77 Massachusetts Avenue, Cambridge, Ma 02139.
[8] M. Aoki, K. Hagiwara, and N. Okamura, Phys. Lett. B **554**, 121 (2003).
[9] A. de Bellefon *et al.*, arXiv:hep-ex/0607026.
[10] V. Barger *et al.*, arXiv:0705.4396.
[11] J. F. Beacom and M. R. Vagins, Phys. Rev. Lett. **93**, 171101 (2004).
[12] H. Watanabe *et al.* (Super-Kamiokande Collaboration), arXiv:0811.0735.
[13] S. Dazeley, A. Bernstein, N. S.Bowden, and R. Svoboda, Nucl. Instrum. Methods Phys. Res., Sect. A **607**, 616 (2009).
[14] P. Vogel and J. F. Beacom, Phys. Rev. D **60**, 053003 (1999).
[15] R. Gandhi *et al.*, Phys. Rev. D **76**, 073012 (2007).
[16] R. Lazauskas and C. Volpe, Nucl. Phys. **A792**, 219 (2007).
[17] W. C. Haxton, Phys. Rev. D **36**, 2283 (1987).
[18] L. B. Auerbach *et al.* (LSND Collaboration), Phys. Rev. D **63**, 112001 (2001).
[19] W. C. Haxton, Phys. Rev. C **37**, 2660 (1988).
[20] T. Adams *et al.* (NuSOnG Collaboration), Int. J. Mod. Phys. A **24**, 671 (2009).
[21] Y. Ashie *et al.* (Super-Kamiokande Collaboration), Phys. Rev. D **71**, 112005 (2005).